Improved Head and neck contrast enhanced imaging using high resolution isotropic 3D T1 SPACE: A feasibility study

M. Viallon[1], K. Masterson[1], and M. Becker[1]
[1]Radiologie, Hopital Universitaire de Genève, Geneva, Switzerland

Introduction

Post Gadolinium MR head and neck examinations remain challenging due to the need for a large anatomic coverage in minimum acquisition time. For cranial nerves and skull base investigations, 3D acquisitions are very useful not only to better visualize and analyze the cranial nerves but also to provide large head and neck coverage of wide-spread or multi-focal pathology. Until recently, 3D acquisitions implemented to image the head and neck area were based on a gradient echo imaging kernel (T1 3D Vibe FS, T1 MP-RAGE [1-3]. Unfortunately, fast 3D T1w gradient echo imaging is limited by the presence of air-tissue interfaces and inherent susceptibility artifacts. Nevertheless, to study the entire course of cranial nerves and localize focal or global contrast enhancement, a fat saturated spin-echo 3D T1 sequence seems more adequate. The purpose of our study was to investigate the utility of a 3D T1 FS Space (**S**ampling **P**erfection with **A**pplication optimized **C**ontrasts using different flip angle **E**volutions) [4] for head and neck imaging at 3T and its clinical relevance in various pathologies of this region.

Materials and Method

30 patients with a variety of benign and malignant pathologic conditions affecting the head and neck area were included in a prospective imaging protocol on a 3T Trio MRI scanner (Siemens, Erlangen, Germany). The protocol consisted of standard 2D sequences (contrast enhanced axial T1 weighted TSE FS and/or T1 3D vibe FS sequence) followed by an additional 3D T1 FS SPACE sequence. For the head and neck protocol, a 12 elements head-neck coil was used, with an additional 4 elements surface coil (Machnet B.V., Eelde, Netherlands) to enforce signal covering the area of the mandible and inner ear, respectively. For head imaging a 32 elements head-coil was generally preferred provided patient head-size and/or patient compliance are compatible with the coil size. The 3D T1 FS SPACE sequence [4] was modified to allow maximized T1 weighting with fat saturation contrast (spectral saturation) at 3T. Main MR parameters for our T1 weighted sequences were: TE/TR/BW=9.4ms/993-1050/849Hz/pixel, voxel=0.9mm^3. Parallel acquisition (iPAT factor=2) and variable flip angles along the echo train (DP var mode) were used. T1 weighting of the designed sequence was compared to existing T1 weighted clinical and already published sequences (T1 TSE FS, T1 SE FS and T1 3D VIBE FS) by imaging a phantom consisting in 25 tubes filled with agar gel of varying Gadolinium concentrations. Two values of TR for the T1 FS 3D SPACE sequence were tested: TR1=993ms and TR2=1150ms. Based on our clinical experience, despite using a variable flip angle as a refocusing RF pulse the specific absorption rate (SAR) at 3T imposed very often an increase of TR between 993ms and 1150ms. Each 3D T1 FS SPACE acquisition consisted of a large sagittal stack with an anterior-posterior phase encoding direction and around 192 partitions. For each patient, multiplanar reconstruction reformatted coronal, oblique and/or curvilinear 3D datasets were obtained. The 3D datasets were analyzed using simple MPR, MIP or MINIP reconstruction. Thin MIP or thin MINIP were additionally obtained in any orientation depending on the region of interest.

Results

Fig1. show that the SNR measurements: trends of the T1 FS 3D SPACE sequence are similar to those of all reference tested sequences. As expected the two T1 FS 3D SPACE offer a much better signal to noise ratio (SNR), the highest SNR is obtained for longest TR (TR2=1150ms), then for shortest TR (TR1=993ms), then TSE, SE and VIBE.

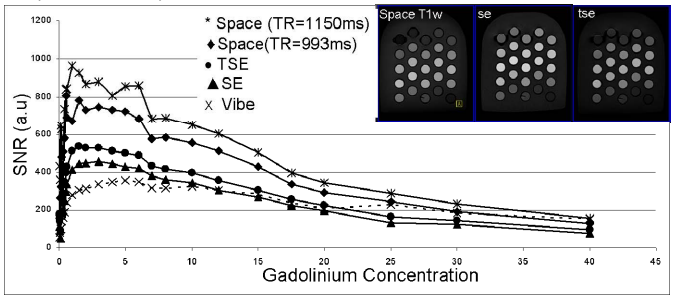

Fig1.SNR measurements obtained on a phantom made from several tubes of Gadolinium with concentration varying between 0 and 40 (T1 values between 7.2 and 2357 ms; T2 values between 9 and 108ms; T1/T2 values between 0.55 and 21.8) for the T1 3D FS SPACE, T1 3D FS VIBE ,SE and TSE sequences.

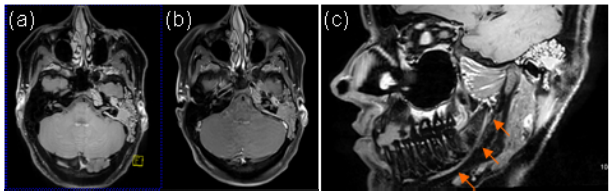

Fig2. (a-b) Contrast enhanced (ce) T1 3D FS space vs T1 FS TSE in a patient with a tumour in the left internal auditory canal; (c) curved MPR showing the mandibular nerve course(orange arrows).

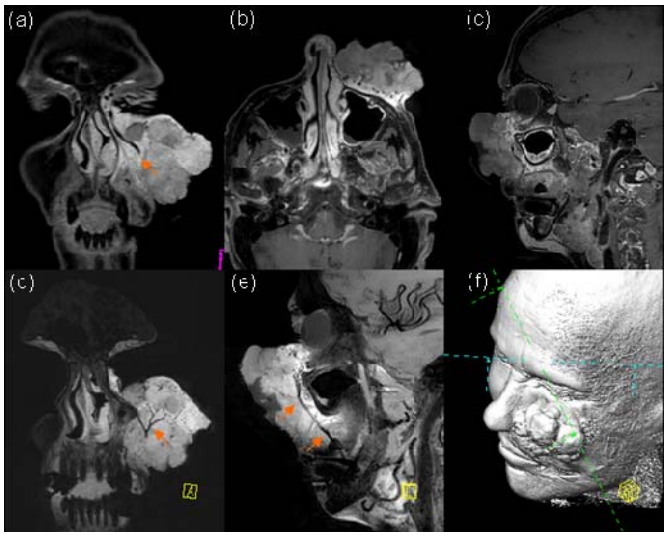

Fig3. Contrast enhanced (ce) T1 3D FS space images obtained on a patient with a large melanoma of the left cheek. (a-c) MPR images (d-e) Thin MINIP reconstruction showing vessels feeding the tumor (orange arrow). (f) Surface rendering obtained from 3D dataset showing the tumor location

Discussion and Conclusion

High quality imaging of the head/neck and maxillofacial area without image distortion and with excellent homogenous fat saturation of the entire examined region is possible using the T1 3D FS Space sequence. The T1 3D FS Space sequence has an increased capacity to depict the anatomy and a variety of benign and malignant lesions of the head-neck as compared to conventional 2D acquisitions. The T1 3D FS Space sequence enables accurate identification of the number of lesions and precise assessment of their spatial extension within and along the nerve tracts and skull base. The anatomical coverage offered by the 3D acquisition, and the ability to slice through the volume of interest enables precise analysis of a lesion and its impact on adjacent cranial nerves and/or vessels. The sequence is very useful in the evaluation of tumoral pathology since nerve distortion and/or compression by neoplasms can be nicely displayed by thin MIP and curved MPR. The 3D T1 FS Space sequence may also be helpful in the analysis of nerve entrapment and nerve compression syndromes by precisely detecting the compression sites. Pre-surgical planning of skull base lesions could also benefit from the T1 3D FS Space sequence due to accurate registration since distortions are the main disadvantages of standard MR sequences for surgical pre-planning [5]

References: (1) Aagaard, B. D., K. R. Maravilla, et al. (1998). Magn Reson Imaging Clin N Am 6(1): 179-94. (2) Makabe, T., M. Nakamura, et al. (2009). Nippon Hoshasen Gijutsu Gakkai Zasshi 65(7): 945-51. (4) Wetzel, S. G., G. Johnson, et al. (2002). AJNR Am J Neuroradiol 23(6): 995-1002. (4) Lichy, M. P., B. M. Wietek, et al. (2005). Invest Radiol 40(12): 754-60. (5) Tanner, S. F., D. J. Finnigan, et al. (2000). Phys Med Biol 45(8): 2117-32.